Impact of DLC Coating Deposition on the Fatigue Strength of Al-7075-T6 Aluminum Alloy

Emanuele Vincenzo Arcieri* and Sergio Baragetti

Department of Management, Information and Production Engineering, University of Bergamo, Viale Marconi 5, Dalmine 24044, Italy

Abstract: Al-7075 has interesting mechanical properties but is susceptible to corrosion. Physical Vapor Deposition (PVD) of coatings results in good corrosion resistance and compressive stresses of the order of 1 GPa on the surface of metallic components. However, the impact of PVD films on the strength of Al-7075-T6 is uncertain. This paper provides a summary of the findings of the Authors' research group in recent years on the fatigue behavior of Al-7075-T6 with and without PVD Diamond-like Carbon (DLC) coating. The results indicated that DLC-coated specimens have lower fatigue strength than uncoated specimens for lives up to about 10000000 cycles. The failure mechanism was determined by observation of the fracture surfaces of the failed specimens. The stress analysis performed confirms the experimental observation, with crack nucleation expected below the surface of coated specimens, where the highest tensile stresses occur during fatigue loading.

Keywords: Fatigue, Al-7075-T6, DLC coating, Experimental tests, Fracture surface observation, Stress analysis.

1. INTRODUCTION

Aluminum is the second most common metallic material in the world and it has a density that is roughly one-third that of steel. Some alloys, such as pure aluminum, are characterized by poor mechanical properties, while others are stronger than structural steels. Aluminum has good corrosion resistance in various environments and appreciable machinability. Thanks to these qualities, aluminum alloys are employed in a variety of applications, including building, construction, automotive, aerospace, aviation, and marine industries [1-3]. Sheets, plates, foils, rods, wires, pipes, extruded shapes, impact castings, forgings, and stampings are all possible product forms of aluminum and its alloys. Powder metallurgy can be used to manufacture components and obtain composites [4]. Aluminum parts can be fastened by bolts and rivets, and can also be welded, although it is necessary to avoid leaving oxide fragments in the weld, which could reduce its ductility and increase the likelihood of cracking. Due to their lower weldability associated with the high thermal conductivity, aluminum alloys must be heated significantly more quickly than steel. Distortions may be brought on by the high coefficient of thermal expansion and high thermal conductivity [1].

According to the nomenclature of the Aluminum Association, the major alloying element in the 7xxx aluminum series is zinc. However, other alloying elements such as copper, magnesium, chromium, and zirconium can be present. In the 7xxx series, the strength ranges from good to extremely good. In the case of high strengths, the resistance to stress corrosion cracking is reduced and over-aging is required. The second digit in an alloy designation, which varies from 1 to 9, denotes alterations to the original alloy while the other digits are merely used to identify the alloys and have no additional significance. Alloys of aluminum are commonly identified by their temper. Designations are made using a capital letter to indicate a fundamental temper and, if necessary, a possible string of digits to indicate certain treatment sequences and their variations. Even if the temper is the same between different alloys, time, temperature, and other heat-treatment parameters can differ. The letter T stands for a solution heat-treatment, *i.e*. a stable temper, for alloys whose strength is stable within a few weeks of solution treatment and T6 stands for solution heat-treatment and artificial aging. Precipitation causes grain refinement, solid solution strengthening, precipitation hardening, and dislocation hardening, which lead to improved mechanical properties [1, 5-7].

Al-7075 has the highest strength of any aluminum alloy, strong fracture toughness, and medium machinability [8]. The ultimate tensile strength (UTS) and yield stress (YS) of Al-7075-T6 are typically UTS = 524 MPa and YS = 462 MPa [9] even if higher tensile strength was measured in [10], with UTS = 648 MPa and YS = 547 MPa, and in [11], with UTS = 650 MPa and YS = 598 MPa. The chemical composition of

*Address correspondence to this author at the Department of Management, Information and Production Engineering, University of Bergamo, Viale Marconi 5, Dalmine 24044, Italy; Tel: +39 0352052382;
E-mail: emanuelevincenzo.arcieri@unibg.it

E-ISSN: 2410-4701/23

Al-7075 is as follows (wt. %): 1.20 - 2.00 % Cu, 2.10 - 2.90 % Mg, ≤ 0.30 % Mn, ≤ 0.40 % Si, ≤ 0.50 % Fe, 0.18 - 0.28 % Cr, 5.1 - 6.1 % Zn, ≤ 0.20 % Ti, ≤ 0.05 % other elements (≤ 0.15 % in total). Al-7075 has a density of 2.80 g cm^{-3} at 20 °C and is used for high strength structural parts in aeronautical field [8]. Inclusions or intermetallic phases close to the surface of components could act as crack nucleation sites [12]. Al-7075-T6 is prone to corrosion fatigue and stress corrosion cracking [13-15].

Corrosion [16], impact damage [17, 18], stress concentrations [19], fatigue [20, 21] and some combinations [22] are common causes of failure in mechanical components. The deposition of coatings can boost the tribological properties and provide corrosion protection [23-29]. In particular, Physical Vapor Deposition (PVD) coatings have very high hardness (up to over 3000 HV), excellent surface finishing, and strong chemical and thermal durability. They can be deposited on a variety of metals with a process temperature range of 150–500 °C [30]. The deposition process, in conjunction with the thermal expansion difference between the coated material and the coating, as well as their structural and interfacial mismatch, creates compressive stresses of the order of 1 GPa on metallic components [10, 11, 31, 32]. If the deposited layer is free from defects, and does not delaminate, these compressive stresses are expected to improve fatigue life [33-39]. However, it has been observed that the deposition of a coating reduces the strength of aluminum components [40] while has little effect on the fatigue resistance of steel components [41, 42].

The impact of PVD coating deposition on the strength of Al-7075-T6 is debatable. The thermal loads that are applied during the deposition process cause microstructural alterations that reduce the fatigue resistance of the substrate. This behavior was observed, for instance, after ZrN and TiN coatings were deposited at high temperatures (>400 °C) [10, 43, 44]. However, even the low temperature deposition of a WC/C coating reduces the fatigue strength of Al-7075-T6 [11, 45]. On the other hand, Puchi-Cabrera *et al*. [46] found positive outcomes for Al-7075-T6 coated with an electroless Ni-P coating under fatigue loading. High shear stresses can result from the difference between the elastic and hardness properties of the Al-7075-T6 substrate and the deposited coating. These stresses can lead to coating delamination and reduce the component fatigue resistance as noted by Elambasseril and Ibrahim [47] and Oskouei *et al*. [48] for TiN, by Baragetti *et al*. [11] for WC/C and by Puchi-Cabrera *et al*. [10] for ZrN. According to Puchi-Cabrera *et al*. [10] and Baragetti *et al*. [11], coating cracking and delamination take place at low fatigue lives, which correspond to high applied stresses.

The PVD process can be used to apply a Diamond-Like Carbon (DLC) coating. This coating is frequently used on tools and machine parts because it has good adhesion capability to various alloys [49, 50]. DLC is a metastable structure of amorphous carbon with graphite- and diamond-like bonds and adsorbed hydrogen. It commonly ensures high modulus of elasticity, high hardness, low surface roughness, high wear resistance and high corrosion protection [51-55] even if the chemistry affects these properties [56-58] and the tensile strength is modified at high temperatures [59, 60]. Due to the possible presence of defects in the coating which can induce corrosion [61], a multilayer design must be preferred [62].

Due to the importance of Al-7075-T6 and DLC coatings in industrial applications, this paper provides a synthesis of the results obtained by the Authors' research group in recent years on the fatigue behavior of uncoated and DLC-coated specimens made of Al-7075-T6. The results show reduced fatigue strength of coated specimens versus uncoated specimens for fatigue lifetimes up to approximately 10000000 loading cycles. Observation of the fracture surfaces of the failed specimens and stress analysis were used to identify the mechanisms that caused the failure.

2. FATIGUE OF AL-7075-T6 IN THE ABSENCE AND PRESENCE OF A DLC COATING

Unlike low carbon steel, the S-N curves of aluminum and its alloys have no fatigue limit, *i.e*. the maximum allowable alternating stress always varies with the number of cycles. The chemical composition and microstructure of the material, the amount of oxygen existing, the temperature, and the component's processing affect the crack propagation rate [7].

The fatigue strength of uncoated and DLC-coated Al-7075-T6 samples under rotating bending is described in [63]. Magnetron sputtering was used to deposit the DLC coating [64], with a maximum temperature of only 180 °C. A low deposition temperature prevents a significant decline in the substrate mechanical properties, which is supported by the absence of changes in the Al-7075-T6 crystal structure following the coating deposition. The resulting coating is extremely stiff and hard and it has a bi-layer architecture that increases adhesion capacity [31]. The surfaces of the specimens were diamond polished before the coating deposition as it was observed that coatings adhere better on diamond polished specimens than specimens polished with 1200 grit paper [65].

A rotating bending testing machine was used to conduct the fatigue tests according to the step loading method [66], which consists of a series of load blocks with constant amplitude applied to each specimen in sequence (Figure **1**). Each load block is of Nlife cycles, where Nlife is the fatigue life at which the load at failure is sought. If the specimen failure does not occur during one load block, the applied load is raised in the following one. A linear interpolation (Equation **1**) between the nominal stress range applied to the specimen in the failure load block, Sf, and the nominal stress range applied in the last unfailed load block, Sp, can be used to evaluate the nominal stress range S* providing a fatigue life of Nlife loading cycles, given the number of cycles Nf ≤ Nlife at which the specimen fails in the failure load block:

$$S^* = Sp + \frac{Nf}{Nlife}(Sf - Sp) \quad (1)$$

Results obtained with the step loading method are within the statistical range of conventional S-N curves [67]. For the investigated fatigue lives, two specimens were used: the first to calculate the stress at failure and the other to validate the obtained result. The confirmation specimen was loaded with the stress S* obtained with the first specimen and if it did not fail another test was performed using the step loading technique. The average value of the stresses obtained with the two tests was assumed as the stress at failure for the considered fatigue life Nlife.

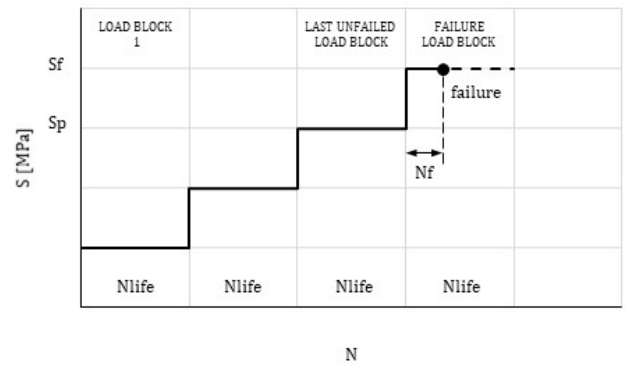

Figure 1: Scheme of the step loading procedure, described in [66].

The results of the experimental tests are reported in Figure **2**, adapted from [63]. The data points represented by triangles are taken from [68], while the others are taken from [69-72]. Black triangles and circles refer to uncoated specimens (denoted as "u"), while white symbols refer to DLC-coated specimens (denoted as "d"). In the 200000 – 10000000 cycle range, DLC deposition appears to be the cause of an

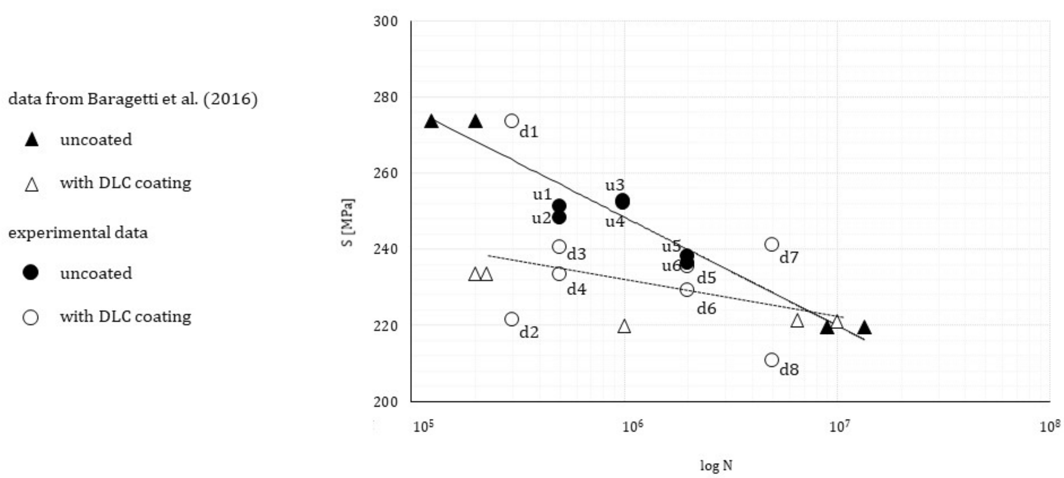

Spec.	u1	u2	u3	u4	u5	u6	d1	d2	d3	d4	d5	d6	d7	d8
Nf	101123	507355	74007	79160	1606118	550038	48543	167638	32049	325728	1830631	1083723	433929	223033
Sf	255	248	275	260	240	239	290	230	245	235	230	240	250	220
S*	251	248	252	253	238	236	273	221	240	233	229	235	241	211

Figure 2: Results of rotating bending tests on uncoated and DLC-coated specimens made of Al-7075-T6. Figure adapted from [63], data from [68-72].

overall decline in Al-7075-T6 fatigue resistance. According to Baragetti *et al*. [73], the thermal load applied during the coating deposition process is the main responsible for this drop. The slope of the S-N curve of the coated samples is lower than that of the uncoated ones due to the small thermal load applied during the deposition of the coating and the advantageous compressive state of the order of 1 GPa induced in the coating [31, 73], leading to a match of the two curves at about 10000000 cycles. The strength of the coated and untreated specimens is therefore comparable for fatigue lives between 1000000 and 10000000 cycles.

Figure **3** (adapted from [63, 70-72]) depicts some typical fracture surfaces of the tested specimens. Figures **3a** to **c** show the surfaces of the uncoated sample u1 which failed after 101123 cycles with an applied stress of 255 MPa, of the coated sample d8 that failed after 223033 cycles with an applied stress of 220 MPa (middle stress level), and of the coated sample d1 that failed after 48543 cycles with an applied stress of 290 MPa (high stress level). In the diagram, N, P, and F stand for the nucleation sites, propagation areas, and final failure areas, respectively. According to Figure **3a** a single crack propagated in the specimen u1. Such a failure mechanism may be caused by the steep stress gradient produced by the high bending moment applied on the specimen and by any imperfections introduced by the polishing processes. In contrast to the specimen d1 that failed at 290 MPa, which seems to have several cracks, the coated sample d8 shows only one crack nucleation site below the sample surface (Figures **3b** and **c**). The low magnification of Figure **3c** prevents a precise identification of the nucleation points and the propagation region in the fracture surface of the specimen d1 and therefore in Figure **3c** only the failure area is indicated. Such fracture surfaces are common when high load amplitudes are applied and stress concentrations are present [74]. The flake in Figure **3c** highlights the high plastic strain undergone by the specimen before the failure.

The location of possible crack nucleation points in the coated samples in the case of uniform defect distribution can be obtained by stress analysis (Figure **4**, adapted from [63, 71, 72]). The distribution of the total stresses in the coated specimens during the experimental tests is given by the sum of the residual stresses associated with the deposition of the coating to the stresses induced by the application of the bending moment. Considering a stress field of the type presented in [36], a residual compressive stress of the order of 1 GPa occurs on the surface of the specimen, while the maximum tensile stress occurs at about 0.1 mm below the surface. The highest bending stresses occur near and on the external surface of the specimen, at the minimum cross section. Since the applied bending stresses are very low compared to the residual compressive residual stress on the surface of all specimens tested, the total stress is compressive on the external surface and the maximum total stress is again at approximately 0.1 mm from the external surface of the coated specimens. As a result, crack nucleation is expected to occur below the surface of the coated specimens, where the highest tensile stresses are present, as confirmed by the observation of the fracture surfaces of the tested specimens. However, high compressive stresses in the coating can cause spallation resulting in decreased strength of the specimens.

3. CONCLUSIONS

The recent findings of the Authors' research group on the fatigue behavior of Al-7075-T6 with and without DLC coating are summarized in this paper. For lifetimes up to approximately 10000000 loading cycles,

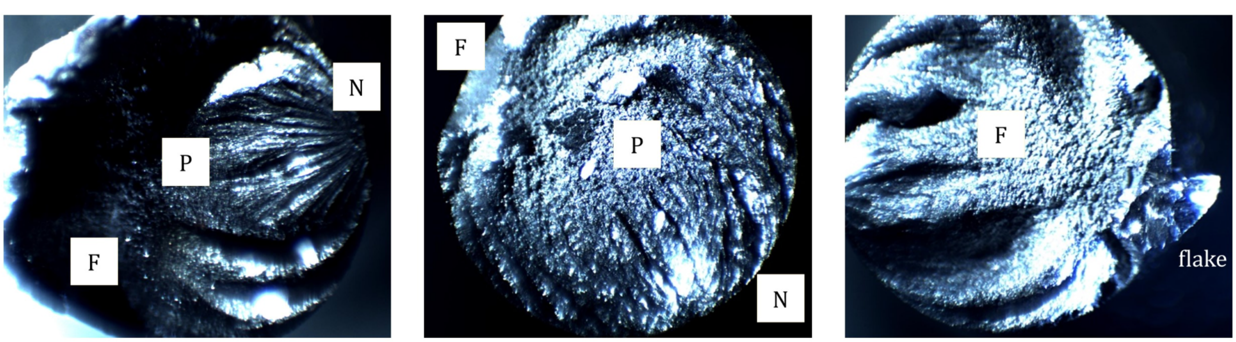

a) b) c)

Figure 3: Fracture surfaces of specimens u1, d8 and d1. Figure adapted from [63, 70-72].

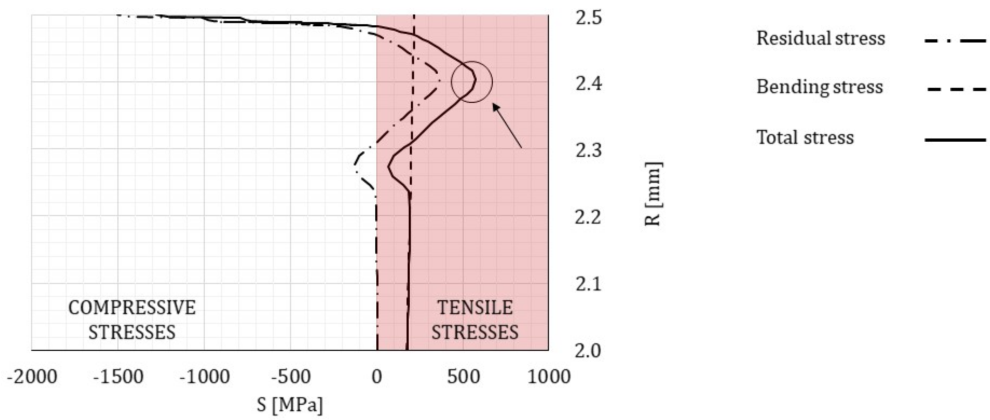

Figure 4: Stress analysis for a DLC-coated specimen. Figure adapted from [63, 71, 72].

DLC-coated specimens have lower fatigue strength than untreated specimens. Failure in the uncoated specimens may be caused by the high stress gradient due to the high bending moment applied on the specimens and by any flaws introduced during the polishing activities. Coated samples which failed at middle stress levels show only one crack nucleation site under the sample surface, while specimens failed at high stress levels exhibit multiple crack nucleation points. Stress analysis supports the fracture surface observation: the crack nucleation is expected to occur below the surface of the coated specimens, where the highest total stresses occur.

REFERENCES

[1] Rooy, E.L., 1990. Introduction to aluminum and aluminum alloys, properties and selection: Nonferrous alloys and special-purpose materials, Vol. 2, ASM Handbook, By ASM Handbook Committee, ASM International, p. 3-14. https://doi.org/10.31399/asm.hb.v02.a0001057

[2] Feng, T., Ma, B., Chen, F., Zhan, L., Xu, Y., Yang, C., 2022. The effect of temperature on the creep ageing characteristics of Al-Li alloys. Journal of Material Science and Technology Research 9: 65-73. https://doi.org/10.31875/2410-4701.2022.09.07

[3] Li, D., Han, L., Chrysanthou, A., Shergold, M., 2018. Influence of corrosion of self-piercing riveted high strength aluminium alloy joints with button cracks on the mechanical strength. Journal of Material Science and Technology Research, 5: 16-27. https://doi.org/10.31875/2410-4701.2018.05.4

[4] Su, Y., Yang, J., Lin, Z., Qiu, C., Chai, X., Liu, X., Cao, H., Wang, Ouyang, Q., 2022. Structural modeling and thermal conductivity of graphite film reinforced aluminum matrix laminated composites. Journal of Material Science and Technology Research 9: 34-42. https://doi.org/10.31875/2410-4701.2022.09.04

[5] Cayless, R.B.C., 1990. Alloy and temper designation systems for aluminum and aluminum alloys, properties and selection: Nonferrous alloys and special-purpose materials, Vol. 2, ASM Handbook, By ASM Handbook Committee, ASM International, p. 15-28. https://doi.org/10.31399/asm.hb.v02.a0001058

[6] Panigrahi, S.K., Jayaganthan, R., 2011. Effect of ageing on microstructure and mechanical properties of bulk, cryorolled, and room temperature rolled Al Al-7075 alloy. J. Alloy. Compd. 509: 9609-9616. https://doi.org/10.1016/j.jallcom.2011.07.028

[7] Bray, J.W., 1990. Aluminum mill and engineered wrought products, properties and selection: Nonferrous alloys and special-purpose materials, Vol. 2, ASM Handbook, By ASM Handbook Committee, ASM International, p. 29-61. https://doi.org/10.31399/asm.hb.v02.a0001059

[8] VVAA, 1990. Properties of wrought aluminum and aluminum alloys, properties and selection: Nonferrous alloys and special-purpose materials, Vol. 2, ASM Handbook, By ASM Handbook Committee, ASM International, p. 62-122. https://doi.org/10.31399/asm.hb.v02.a0001060

[9] Matweb, www.matweb.com.

[10] Puchi-Cabrera, E.S., Staia, M.H., Lesage, J., Gil, L., Villalobos-Gutiérrez, C., Barbera-Sosa, J.L., Ochoa-Pérez, E.A. and Bourhis, E.L., 2008. Fatigue behavior of AA7075-T6 aluminum alloy coated with ZrN by PVD. Int. J. Fatigue 30: 1220-1230. https://doi.org/10.1016/j.ijfatigue.2007.09.001

[11] Baragetti, S., Gerosa, R., Villa, F., 2016. Step loading corrosion fatigue testing of 7075-T6 WC/C coated specimens in air and methanol. Eng. Fract. Mech. 164: 106-116. https://doi.org/10.1016/j.engfracmech.2016.02.027

[12] Leng, L., Zhang, Z.J., Duan, Q.Q., Zhang, P., Zhang, Z.F., 2018. Improving the fatigue strength of 7075 alloy through aging. Mat. Sci. Eng. A 738: 24-30. https://doi.org/10.1016/j.msea.2018.09.047

[13] Silva, G., Rivolta, B., Gerosa, R., Derudi, U., 2013. Study of the SCC behavior of 7075 aluminum alloy after one-step aging at 163 °C. J. Mater. Eng. Perform. 22: 210-214. https://doi.org/10.1007/s11665-012-0221-4

[14] Brown, B. F., 1972. Stress-corrosion cracking in high strength steels and in titanium and aluminum alloys, Naval Research Laboratory: Washington, D.C.

[15] Sankaran, K.K., Perez, R., Jata, K.V., 2001. Effects of pitting corrosion on the fatigue behavior of aluminum alloy 7075-T6: modeling and experimental studies. Mater. Sci. Eng. A 297(1-2): 223-229. https://doi.org/10.1016/S0921-5093(00)01216-8

[16] Baragetti, S., Borzini, E., Arcieri, E.V., 2018. Effects of environment and stress concentration factor on Ti-6Al-4V specimens subjected to quasi-static loading. Procedia Struct. Integr. 12: 173-182. https://doi.org/10.1016/j.prostr.2018.11.097

[17] Arcieri, E.V., Baragetti, S., Božić, Ž., 2021. Application of design of experiments to foreign object damage on 7075-T6. Procedia Struct. Integrity 31: 22-27. https://doi.org/10.1016/j.prostr.2021.03.005

[18] Baragetti, S., Arcieri, E.V., 2019. Study on a new mobile anti-terror barrier. Procedia Struct. Integr. 24: 91-100. https://doi.org/10.1016/j.prostr.2020.02.008

[19] Baragetti, S., Baryshnikov, A., 2001. Rotary shouldered thread connections: Working limits under combined static loading. J. Mech. Des. 123(3): 456-463. https://doi.org/10.1115/1.1371476

[20] Baragetti, S., D'Urso, G., 2014. Aluminum 6060-T6 friction stir welded butt joints: Fatigue resistance with different tools and feed rates. J. Mech. Sci. Technol. 28(3): 867-877. https://doi.org/10.1007/s12206-013-1152-1

[21] Baragetti, S., Guagliano, M., Vergani, L., 2000. Numerical procedure for shot peening optimization by means of non-dimensional factors. Int. J. Mater. Prod. Technol. 15(1): 91-103. https://doi.org/10.1504/IJMPT.2000.001238

[22] Baragetti, S., 2013, Corrosion fatigue behaviour of Ti-6Al-4V in methanol environment. Surf. Interface Anal. 45(10): 1654-1658. https://doi.org/10.1002/sia.5203

[23] Brioua, S., Belmokre, K., Debout, V., Jacquot, P., Conforto, E., Touzain, S., Creus, J., 2022. Influence of spray parameters on the metallurgical and functional properties of HVOF WC based cermets deposited onto low alloy steel. Journal of Material Science and Technology Research 9: 1-10. https://doi.org/10.31875/2410-4701.2022.09.01

[24] Yaqoob, S., Hasan, N., Khalid, S., Akhtar, M. S., 2022. Structural, morphological and optical study of manganese doped FeS (Mackinawite) nanostructures by chemical bath deposition (CBD) technique. Journal of Material Science and Technology Research 9: 24-33. https://doi.org/10.31875/2410-4701.2022.09.03

[25] Silva, T., Ferreira, M., Nascimento, J., Pietro, L., Neto, L. C., Moreira, H., Pereira, L., Leite, N., Gelamo, R., Moreto, J. A., 2022. Development of a low-cost ball-on-flat linear reciprocating apparatus: test validation using Ti-6Al-4V and Ti-6Al-4V/Nb2O5 coatings. Journal of Material Science and Technology Research, 9: 43-52. https://doi.org/10.31875/2410-4701.2022.09.05

[26] Baragetti, S., 2022. Numerical and experimental investigation of the effects of thin hard coatings on the strength of spur gears. Journal of Material Science and Technology Research, 9: 74-86. https://doi.org/10.31875/2410-4701.2022.09.08

[27] Loperena, A., Lehr, I., Saidman, S., 2021. Electrosynthesis of a duplex coating consisting of a cerium-based layer and a polypyrrole film for the corrosion protection of AISI 304 stainless steel. Journal of Material Science and Technology Research, 8: 1-11. https://doi.org/10.31875/2410-4701.2021.08.1

[28] Yan, G., Xiaobing, S., Weiqiang, P., Zhao, Q., Huixiang, X., Huan, L., Xuezhong, F., 2021. Surface coating of Cyclotetramethylenetetranitramine (HMX) particles and its property investigation. Journal of Material Science and Technology Research, 8: 77-81. https://doi.org/10.31875/2410-4701.2021.08.9

[29] Loskutov, S., Ershov, A., Zelenina, E., 2020. Strength and mechanism of adhesion to the substrate layer while applying plasma coatings in oxidizing environments. Journal of Material Science and Technology Research, 7: 1-10. https://doi.org/10.31875/2410-4701.2020.07.01

[30] Bull, S.J., 2006. Physical vapour deposition methods for protection against wear, in: Mellor, B.G. (Ed.), Surface coatings for protection against wear, Woodhead Publishing Ltd., Abington, UK, p. 146. https://doi.org/10.1533/9781845691561.146

[31] Srinivasan, N., Bhaskar, L.K., Kumar, R., Baragetti, S., 2018. Residual stress gradient and relaxation upon fatigue deformation of diamond-like carbon coated aluminum alloy in air and methanol environments. Mat. Des. 160: 303-312. https://doi.org/10.1016/j.matdes.2018.09.022

[32] Chang, Y.Z., Tsai, P.H., Li, J.B., Lin, H.C., Jang, J.S.C., Li, C., Chen, G.J., Chen, Y.C., Chu, J.P., Liaw, P.K., 2013. Zr-based metallic glass thin film coating for fatigue-properties. Thin Solid Films 544: 331-334. https://doi.org/10.1016/j.tsf.2013.02.104

[33] Inoue, K., Lyu, S., Deng, G., Kato, M., 1996. Fracture mechanics based evaluation of the effect of the surface treatments on the strength of carburized gears. VDI-Berichte 1320, p. 357.

[34] Su, Y.L., Yao, S.H., Wei, C.S., Wu, C.T., Kao, W.H., 1998. Evaluation on the wear, tension and fatigue behavior of various PVD coated materials. Mater. Lett. 35: 255-260. https://doi.org/10.1016/S0167-577X(97)00259-0

[35] Kim, K.R., Suh, C.M., Murakami, R.I., Chung, C.W., 2003. Effect of intrinsic properties of ceramic coatings on fatigue behavior of Cr-Mo-V steels. Surf. Coat. Technol. 171: 15-23. https://doi.org/10.1016/S0257-8972(03)00229-9

[36] Baragetti, S., La Vecchia, G.M., Terranova, A., 2003. Fatigue behavior and FEM modeling of thin-coated components. Int. J. Fatigue 25: 1229-1238. https://doi.org/10.1016/j.ijfatigue.2003.08.009

[37] Baragetti, S., La Vecchia, G.M., Terranova, A., 2005. Variables affecting the fatigue resistance of PVD-coated components. Int. J. Fatigue 27: 1541-1550. https://doi.org/10.1016/j.ijfatigue.2005.06.011

[38] Gelfi, M., La Vecchia, G.M., Lecis, N., Troglio, S., 2005. Relationship between through-thickness residual stress of CrN-PVD coatings and fatigue nucleation sites. Surf. Coat. Technol. 192: 263-268. https://doi.org/10.1016/j.surfcoat.2004.05.032

[39] Baragetti, S., 2007. Fatigue resistance of steel and titanium PVD coated spur gears. Int. J. Fatigue 29: 1893-1903. https://doi.org/10.1016/j.ijfatigue.2006.11.005

[40] Oskouei, R.H., Ibrahim, R.N., 2011. Restoring the tensile properties of PVD-TiN coated Al 7075-T6 using a post heat treatment. Surf. Coat. Technol. 205: 3967-3973. https://doi.org/10.1016/j.surfcoat.2011.02.041

[41] Baragetti, S., Gelfi, M., La Vecchia, G.M., Lecis, N., 2005. Fatigue resistance of CrN thin films deposited by arc evaporation process on H11 tool steel and 2205 duplex stainless steel, Fatigue Fract. Eng. Mater. Struct. 28: 615-621. https://doi.org/10.1111/j.1460-2695.2005.00905.x

[42] Saini B.S., Gupta, V.K., 2010. Effect of WC / C PVD coating on fatigue behaviour of case carburized SAE8620 steel. Surf. Coat. Technol. 205: 511-518. https://doi.org/10.1016/j.surfcoat.2010.07.022

[43] Oskouei, R.H., Ibrahim, R.N., 2011. The effect of a heat treatment on improving the fatigue properties of aluminium alloy 7075-T6 coated with TiN by PVD. Procedia Eng. 10: 1936-1942. https://doi.org/10.1016/j.proeng.2011.04.321

[44] Oskouei, R.H., Ibrahim, R.N., 2012. An investigation on the fatigue behaviour of Al 7075-T6 coated with titanium nitride using physical vapour deposition process. Mater. Des. 39: 294-302. https://doi.org/10.1016/j.matdes.2012.02.056

[45] Baragetti, S., Gerosa, R., Villa, F., 2014. WC/C coating protection effects on 7075-T6 fatigue strength in an aggressive environment. Procedia Eng. 74: 33-36. https://doi.org/10.1016/j.proeng.2014.06.219

[46] Puchi-Cabrera, E.S., Villalobos-Gutiérrez, C., Irausquín, I., La Barbera-Sosa, J., Mesmacque, G., 2006. Fatigue behavior of a 7075-T6 aluminum alloy coated with an electroless Ni-P deposit. Int. J. Fatigue 28: 1854-1866. https://doi.org/10.1016/j.ijfatigue.2005.12.005

[47] Elambasseril, J., Ibrahim, R.N., 2011. Determination of interfacial fracture toughness of coatings using circumferentially notched cylindrical substrate. Mater. Sci. Eng. A 529: 406-416. https://doi.org/10.1016/j.msea.2011.09.053

[48] Oskouei, R.H., Ibrahim, R.N., Barati, M.R., 2012. An experimental study on the characteristics and delamination of TiN coatings deposited on Al 7075-T6 under fatigue cycling. Thin Solid Films 526: 155-162. https://doi.org/10.1016/j.tsf.2012.11.016

[49] Coldwell, H. L., Dewes, R.C., K. Aspinwall, D., Renevier, N.M., Teer, D.G., 2004. The use of soft/lubricating coatings when dry drilling BS L168 aluminium alloy. Surf. Coat. Technol. 177-178: 716-726. https://doi.org/10.1016/j.surfcoat.2003.08.012

[50] Fukui, H., Okida, J., Omori, N., Moriguchi, H., Tsuda, K., 2004. Cutting performance of DLC coated tools in dry machining aluminum alloys. Surf. Coat. Technol. 187: 70-76. https://doi.org/10.1016/j.surfcoat.2004.01.014

[51] Grill, A., 1993. Review of the tribology of diamond-like carbon. J. Wear 168:143-153. https://doi.org/10.1016/0043-1648(93)90210-D

[52] Hauert, R., 2004. An overview on the tribological behavior of diamond-like carbon in technical and medical applications. Tribol. Int. 37: 991-1003. https://doi.org/10.1016/j.triboint.2004.07.017

[53] Erdemir, A., Donnet, C., 2006. Tribology of diamond-like carbon films: recent progress and future prospects, J. Phys. D: Appl. Phys. 39: R311-R327. https://doi.org/10.1088/0022-3727/39/18/R01

[54] Pu, J., Wang, J., He, D., Wan, S., 2016. Corrosion and tribocorrosion behaviour of superthick diamond-like carbon films deposited on stainless steel in NaCl solution. Surf. Interface Anal. 48: 360-367. https://doi.org/10.1002/sia.5987

[55] Zhao, G., Aune, R.E., Espallargas, N., 2016. Tribocorrosion studies of metallic biomaterials: the effect of plasma nitriding and DLC surface modifications. J. Mech. Behav. Biomed Mater. 63: 100-114. https://doi.org/10.1016/j.jmbbm.2016.06.014

[56] Donnet, C., 1998. Recent progress on the tribology of doped diamond-like and carbon alloy coatings: a review. Surf. Coat. Technol. 100-101: 180-186. https://doi.org/10.1016/S0257-8972(97)00611-7

[57] Donnet, C., Fontaine, J., Grill, A., Le Mogne, T., 2001. The role of hydrogen on the friction mechanism of diamond-like carbon films. Tribol. Lett. 9: 137-142. https://doi.org/10.1023/A:1018800719806

[58] Robertson, J., 2002. Diamond-like amorphous carbon. Mater. Sci. Eng., R. Rep. 37: 129-281. https://doi.org/10.1016/S0927-796X(02)00005-0

[59] Wang, D.-Y., Chang, C.-L., Ho, W.-Y., 1999. Oxidation behavior of diamond-like carbon films. Surf. Coat. Technol. 120-121: 138-144. https://doi.org/10.1016/S0257-8972(99)00350-3

[60] Yang; W.J., Choa, Y.-H., Sekino, T., Shim, K.B., Niihara, K., Auh, K.H., 2003. Thermal stability evaluation of diamond-like nanocomposite coatings. Thin Solid Films 476: 49-54. https://doi.org/10.1016/S0040-6090(03)00466-8

[61] Zeng, A., Liu, E., Zhang, S., Tan, S.N., Hing, P., Annergren, I.F., Gao, J., 2003. Impedance study on electrochemical characteristics of sputtered DLC films. Thin Solid Films 426: 258-264. https://doi.org/10.1016/S0040-6090(02)01289-0

[62] Depner, U., Ellermeier, J., Troßmann, T., Berger, C., Oechsner, M., 2011. The effect of layer structure on corrosion and erosion resistance of thin PVD multilayer films. Int. J. Mater. Res. 08: 1014-1020. https://doi.org/10.3139/146.110548

[63] Baragetti, S., Arcieri, E.V., 2022. Effects of thin hard film deposition on fatigue strength of AA7075-T6, Proc. Inst. Mech. Eng., Part C 236(21): 10713-10722. https://doi.org/10.1177/0954406220980505

[64] Lafer S.p.A., www.lafer.eu

[65] Baragetti, S., Srinivasan, N., Lalithkumar, B., Kumar, R., 2017. Influence of environment, residual stresses on the fatigue behavior of 7075-T6 aluminum alloy. Key Eng. Mater. 754: 3-6. https://doi.org/10.4028/www.scientific.net/KEM.754.3

[66] Nicholas, T., 2002. Step loading for very high cycle fatigue. Fatigue Fract. Engng. Mater. Struct. 25: 861-869. https://doi.org/10.1046/j.1460-2695.2002.00555.x

[67] Bellows, R.S., Muju, S., Nicholas, T., 1999. Validation of the step test method for generating Haigh diagrams for Ti-6Al-4V. Int. J. Fatigue 21: 687-697. https://doi.org/10.1016/S0142-1123(99)00032-8

[68] Baragetti, S., Gerosa, R., Villa, F., 2016. Effects of PVD DLC coating on 7075-T6 fatigue strength at high and low number of cycles. Key Eng. Mater. 713: 50-53. https://doi.org/10.4028/www.scientific.net/KEM.713.50

[69] Arcieri, E.V., Baragetti, S., Borzini, E., 2018. Bending fatigue behavior of 7075-aluminum alloy. Key Eng. Mater. 774: 1-6. https://doi.org/10.4028/www.scientific.net/KEM.774.1

[70] Baragetti, S., Borzini, E., Božić, Ž., Arcieri, E.V., 2019. On the fatigue strength of uncoated and DLC coated 7075-T6 aluminum alloy. Eng. Fail. Anal. 102: 219-225. https://doi.org/10.1016/j.engfailanal.2019.04.035

[71] Baragetti, S., Božić, Ž., Arcieri, E.V., 2020. Stress and fracture surface analysis of uncoated and coated 7075-T6 specimens under rotating bending fatigue loading. Eng. Fail. Anal. 112: 104512. https://doi.org/10.1016/j.engfailanal.2020.104512

[72] Arcieri, E.V., Baragetti, S., 2020. Fatigue behavior of thin hard coated specimens made of 7075. AIP Conference Proceedings 2309: 020027. https://doi.org/10.1063/5.0033959

[73] Baragetti, S., Gerosa, R., Villa, F., 2013. Fatigue behaviour of thin coated Al 7075 alloy with low temperature PVD coatings. Key Eng. Mater. 577-578: 221-224. https://doi.org/10.4028/www.scientific.net/KEM.577-578.221

[74] Milella, P.P., 2013. Fatigue and corrosion in metals, Springer, Milan, Italy. https://doi.org/10.1007/978-88-470-2336-9

Received on 25-02-2023 Accepted on 20-03-2023 Published on 29-03-2023

DOI: https://doi.org/10.31875/2410-4701.2023.10.02